ACS central science

http://pubs.acs.org/journal/acscii

Research Article

Isoprenylcysteine Carboxylmethyltransferase-Based Therapy for Hutchinson–Gilford Progeria Syndrome

Beatriz Marcos-Ramiro, Ana Gil-Ordóñez, Nagore I. Marín-Ramos, Francisco J. Ortega-Nogales, Moisés Balabasquer, Pilar Gonzalo, Nora Khiar-Fernández, Loïc Rolas, Anna Barkaway, Sussan Nourshargh, Vicente Andrés, Mar Martín-Fontecha, María L. López-Rodríguez, and Silvia Ortega-Gutiérrez*

Cite This: *ACS Cent. Sci.* 2021, 7, 1300–1310

Read Online

ACCESS | Metrics & More | Article Recommendations | Supporting Information

ABSTRACT: Hutchinson–Gilford progeria syndrome (HGPS, progeria) is a rare genetic disease characterized by premature aging and death in childhood for which there were no approved drugs for its treatment until last November, when lonafarnib obtained long-sought FDA approval. However, the benefits of lonafarnib in patients are limited, highlighting the need for new therapeutic strategies. Here, we validate the enzyme isoprenylcysteine carboxylmethyltransferase (ICMT) as a new therapeutic target for progeria with the development of a new series of potent inhibitors of this enzyme that exhibit an excellent antiprogeroid profile. Among them, compound UCM-13207 significantly improved the main hallmarks of progeria. Specifically, treatment of fibroblasts from progeroid mice with UCM-13207 delocalized progerin from the nuclear membrane, diminished its total protein levels, resulting in decreased DNA damage, and increased cellular viability. Importantly, these effects were also observed in patient-derived cells. Using the *Lmna*$^{G609G/G609G}$ progeroid mouse model, UCM-13207 showed an excellent in vivo efficacy by increasing body weight, enhancing grip strength, extending lifespan by 20%, and decreasing tissue senescence in multiple organs. Furthermore, UCM-13207 treatment led to an improvement of key cardiovascular hallmarks such as reduced progerin levels in aortic and endocardial tissue and increased number of vascular smooth muscle cells (VSMCs). The beneficial effects go well beyond the effects induced by other therapeutic strategies previously reported in the field, thus supporting the use of UCM-13207 as a new treatment for progeria.

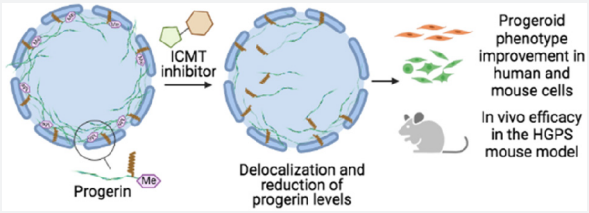

INTRODUCTION

Hutchinson–Gilford progeria syndrome (HGPS), or progeria, is an extremely rare pediatric disorder, characterized by premature aging and death at an average age of 14.6 years.[1−3] The molecular cause of HGPS is an autosomal spontaneous dominant point mutation in the *LMNA* gene (encoding nuclear A-type lamins)[4,5] that leads to the synthesis of progerin, a permanently farnesylated and methylated truncated version of prelamin A.[6] This mutant protein accumulates abnormally in the inner nuclear membrane, causing the multiple and characteristic cellular and organismal alterations of the disease.[1,2]

In November 2020, lonafarnib (Zokinvy), an inhibitor of the enzyme farnesyltransferase aimed at decreasing progerin farnesylation, received the landmark approval by the US Food and Drug Administration (FDA), becoming the first (and only) approved drug for treating progeria. However, the outcome of the lonafarnib clinical trial showed limited benefits,[7] possibly due to alternative prenylation of prelamin A and progerin by geranylgeranyl transferase upon farnesyltransferase inhibition.[8] Yet, treatment of HGPS children with combination therapies inhibiting both prenylation pathways did not seem to improve the benefits achieved with lonafarnib monotherapy.[9] In addition, it is possible that other targets of farnesyltransferase, apart from progerin, are affected by lonafarnib, eliciting adverse effects in progeroid patients. In line with this concern, since lonafarnib was originally developed for the treatment of Ras-dependent tumors,[10] it is antiproliferative, a feature that can potentially limit its positive effects on progeroid cells, in which pro-proliferative effects are needed. Alternative approaches in HGPS animal models have explored the potential use of *N*-acetyltransferase 10 (NAT10) inhibitors,[11] CRISPR/Cas9-based therapy,[12,13] and microbiome-based interventions,[14] but these strategies cannot as yet be easily translated to humans. Finally, a moderate extension of longevity (by 12%) has been reported in the progerin-expressing *Lmna*$^{G609G/G609G}$ mouse model after increasing the levels of ATP and pyrophosphate, but the

Received: December 21, 2020
Published: June 27, 2021

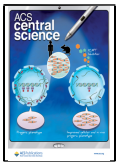

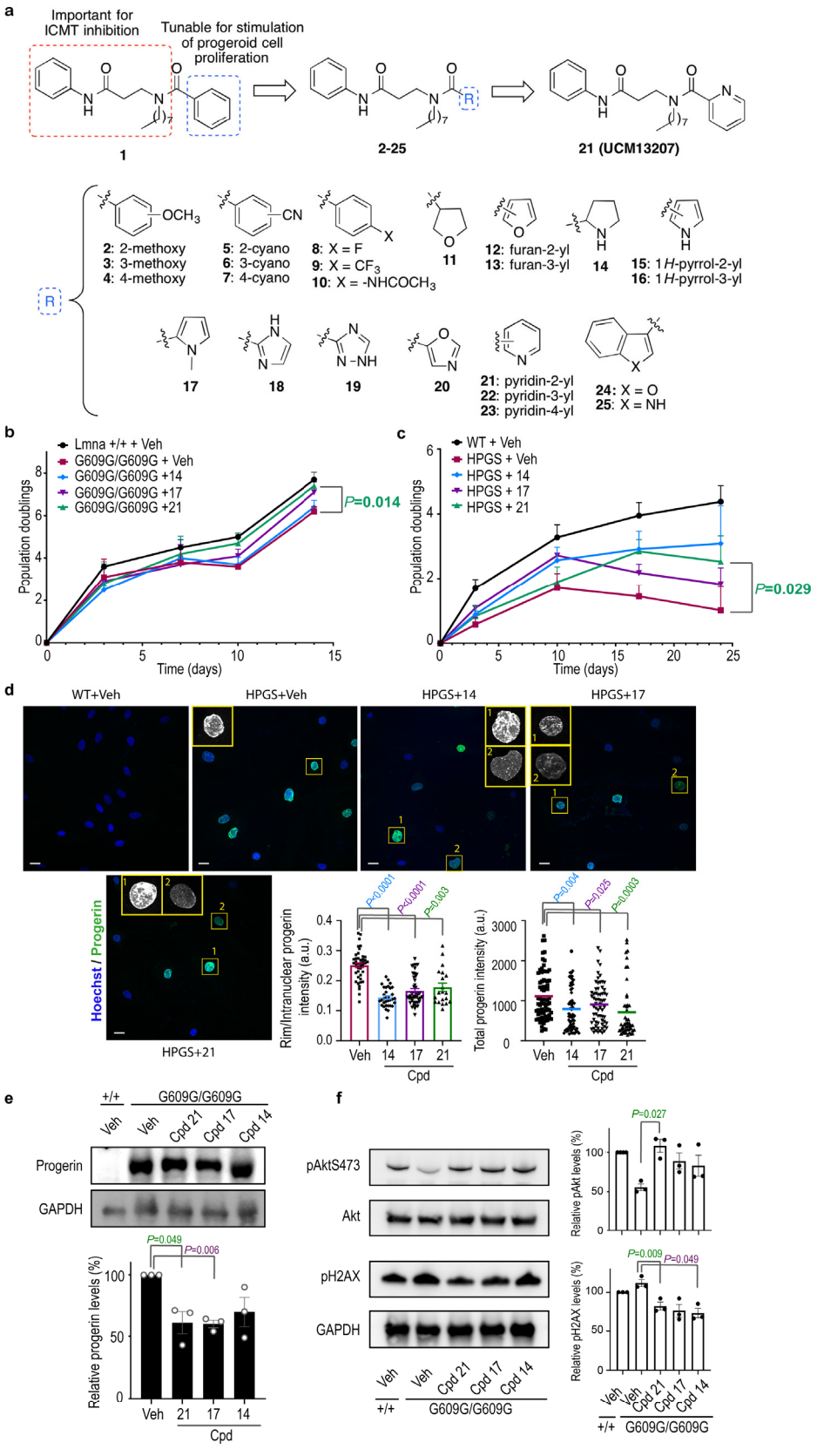

Figure 1. New ICMT inhibitors improve progeria hallmarks in mouse and human HGPS cells. (**a**) Design of new ICMT inhibitors. (**b**) Growth curves of *Lmna*$^{+/+}$ and *Lmna*$^{G609G/G609G}$ mice fibroblasts incubated with 0.1% DMSO (vehicle, veh) or ICMT inhibitors at 10 μM over 14 days ($n \geq 4$ independent experiments; two-tailed Student's *t* test). (**c**) Growth curves of human wild type (WT) or HGPS fibroblasts incubated with vehicle or different ICMT inhibitors at 2 μM over 24 days ($n \geq 4$ independent experiments; two-tailed Student's *t* test). (**d**) Immunofluorescence images of human WT or HGPS fibroblasts treated with vehicle or different ICMT inhibitors at 2 μM for 17 days and stained with antiprogerin (green) and Hoechst (blue). Magnification shows subnuclear distribution of progerin, that was delocalized from the nuclear rim toward the nucleoplasm (1,

https://doi.org/10.1021/acscentsci.0c01698
ACS Cent. Sci. 2021, 7, 1300−1310

Figure 1. continued

quantification in middle plot) and/or decreased (2, quantification in right plot) after treatment with ICMT inhibitors (at least 47 cells quantified per condition from ≥2 independent experiments; two-tailed Student's *t* test). Scale bar: 20 μm. (**e**) Immunoblot of progerin from $Lmna^{+/+}$ or $Lmna^{G609G/G609G}$ mouse fibroblasts incubated with vehicle or ICMT inhibitors (2 μM) for 14 days. Protein levels were normalized against total GAPDH ($n \geq 3$ independent experiments; plot shows mean ± sem, two-tailed Student's *t* test). (**f**) Immunoblot and quantification of phosphorylated Akt (pAkt) and phosphorylated histone 2AX (pH2AX) from $Lmna^{+/+}$ or $Lmna^{G609G/G609G}$ mouse fibroblasts incubated with vehicle or ICMT inhibitors (2 μM) for 14 days. Protein levels were normalized against total Akt or GAPDH, respectively ($n \geq 3$ independent experiments; plots show mean ± sem, two-tailed Student's *t* test).

relevance of this finding to human HGPS remains to be addressed.[15] Hence, there is a clear and urgent need for better therapeutic strategies for treatment of HGPS. Building on the findings that genetic blockade of the enzyme isoprenylcysteine carboxylmethyltransferase (ICMT) ameliorated disease phenotype in the Zmpste24-null mouse model of progeria and in HGPS human cells,[16] we hypothesized that pharmacological inhibitors of ICMT may be beneficial drugs for progeroid patients. Specifically, we considered that small molecule inhibitors of ICMT, an approach previously not explored in progeria, could avoid the carboxymethylation of progerin and consequently induce its delocalization from the nuclear membrane and as such decrease its accumulation, leading to an improvement of HGPS progression. However, the lack of noncytotoxic and bioavailable ICMT inhibitors have to date precluded the therapeutic validation of such a therapeutic strategy. Of note, while the present work was under review, the ability of a previously described ICMT inhibitor to delay senescence of HGPS cells was reported.[17] However, the low bioavailability of this compound has hampered its in vivo assessment. Here, we describe the development of a new potent and selective ICMT inhibitor (compound **21**, UCM-13207) and demonstrate its ability to significantly improve fundamental progeroid features in vitro and in vivo, including increased survival in $Lmna^{G609G/G609G}$ mice. Collectively, our findings indicate that small molecule inhibition of ICMT could be an effective therapy for progeria. Furthermore, as progeria can be considered as an accelerated model of physiological senescence, our findings could have implications for aging-related conditions, one of the major challenges nowadays.[18]

RESULTS AND DISCUSSION

Design and Synthesis of New ICMT Inhibitors. We have previously carried out an extensive medicinal chemistry program aimed at the development of new ICMT inhibitors.[19,20] Based on this work and using the key criteria of potency (80% inhibition at 50 μM) and low cellular toxicity (cellular viability >80% at 10 μM), we selected a new compound (**1**) as our initial hit. Our findings suggested that the 3-amino-*N*-phenylpropanamide moiety as well as the *n*-octyl chain of compound **1** were key elements for interaction with ICMT.[20] Accordingly, we envisioned that the phenyl group could be further explored for optimizing cellular viability without significantly compromising ICMT inhibition (Figure 1a). This focused library was synthesized as detailed in the Supporting Information. In all cases, the obtained structural data were in agreement with the proposed structures (see the Supporting Information for details). All new compounds were screened for ICMT inhibition. In addition, those compounds that blocked >60% of ICMT activity were assayed for cellular viability in mouse wild-type and progerin-expressing fibroblasts ($Lmna^{G609G/G609G}$) (Supporting Table S1). All compounds that showed the strongest capacity to enhance the viability of progeroid fibroblasts (values >70% at 2 μM) were selected for further biological assays with the exception of the furan-containing derivative **13**. The reason for the latter was the narrow efficacy window observed for this compound when tested at a higher concentration (Supporting Figure S1).

New ICMT Inhibitors Improve the Cellular Hallmarks of Progeria in Fibroblasts from $Lmna^{G609G/G609G}$ Mice and HGPS Patients. Next, we sought to confirm whether compounds **14**, **17**, and **21** could counteract some of the most characteristic molecular and cellular defects found in both progeroid mouse and human cells. This included growth arrest, progerin accumulation in the perinuclear rim, Akt inhibition, and increased level of phosphorylated histone 2AX (pH2AX). We found that the three compounds augmented the proliferation rate of progeroid mouse cells (Figure 1b) and, in particular, incubation with compound **21** increased population doubling values almost to the level of $Lmna^{+/+}$ cells. As the $Lmna^{G609G/G609G}$ mouse cells are SV40LT immortalized cells, they are p53 and Rb deficient, and therefore do not undergo senescence. Hence, to rule out the effects of cell immortalization in our results, we confirmed a significant positive proliferative effect of the compounds in primary HGPS human cells (Figure 1c). To further corroborate that the effects regarding the proliferation rate were due to the specific inhibition of ICMT activity, we knocked down its expression and studied the effects of compound **21**. As expected, the effect of the inhibitor in the proliferation rate of progeroid mouse fibroblasts was absent in siRNA-induced ICMT knockout cells, indicating that the beneficial effects exerted by compound **21** are selectively elicited by ICMT inhibition (Supporting Figure S2). Under these conditions, we did not observe a significant effect of the siRNA alone on increasing cellular viability. It is possible that the time point (72 h) and the cells used (immortalized progeroid mouse fibroblasts) are not optimal for observing the direct siRNA effects, which may require longer times to become phenotypically evident, as siRNA and small molecule effect may differ in the extension of the observed effect or the optimal window time. In support of this, published experiments with short hairpin (sh) RNAs of ICMT conducted in human progeroid cells have shown that at least 20 days are needed to observe the effect of the ICMT shRNA alone on cellular viability.[16]

Consistent with their ICMT inhibitory activity, all three compounds induced a significant delocalization of progerin from the nuclear rim in human HGPS cells (Figure 1d, left plot). This effect was accompanied by a decrease in total levels of progerin, as shown by both immunofluorescence experiments using human HGPS cells (Figure 1d, right plot) and by Western blot analysis using mouse progeroid cells (Figure 1e and Supporting Figure S3).

Furthermore, and consistent with the increase in cellular proliferation, phospho-Akt levels were higher in treated

https://doi.org/10.1021/acscentsci.0c01698
ACS Cent. Sci. 2021, 7, 1300−1310

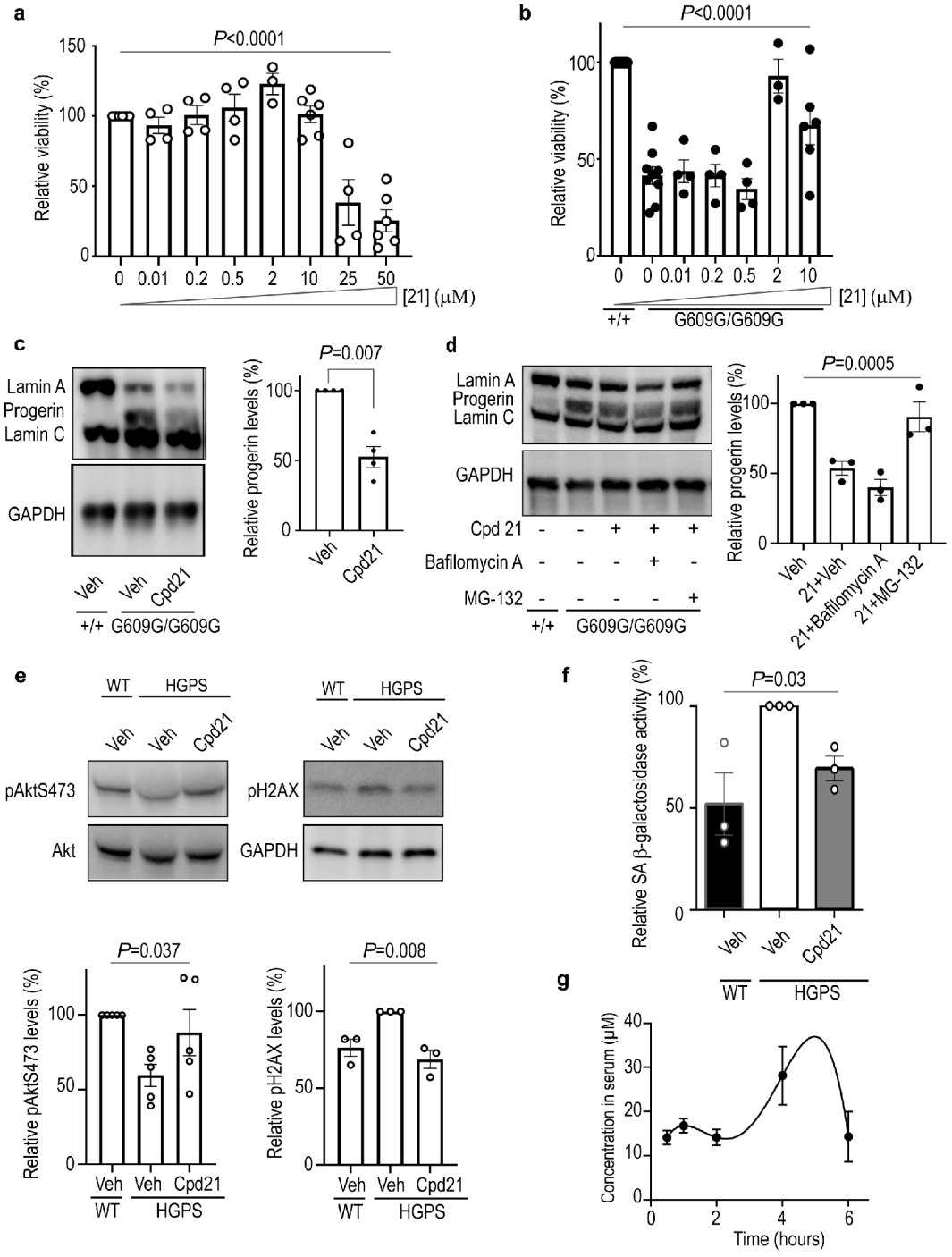

Figure 2. Compound 21 ameliorates the progeria phenotype in mouse and human HGPS fibroblasts. (**a**) $Lmna^{+/+}$ fibroblasts were incubated with compound **21** at different concentrations for 72 h, and viability was determined by an MTT assay ($n \geq 4$ independent experiments; one-way ANOVA). (**b**) $Lmna^{+/+}$ or $Lmna^{G609G/G609G}$ fibroblasts were incubated with compound **21** for 72 h at different concentrations, and viability was assessed by MTT assay ($n \geq 4$ independent experiments; one-way ANOVA). (**c**) Cropped immunoblot of lamin A, progerin, and lamin C from $Lmna^{+/+}$ or $Lmna^{G609G/G609G}$ fibroblasts incubated with 0.1% DMSO (vehicle, veh) or compound **21** at 2 μM for 14 days ($n \geq 3$ independent experiments; plot shows progerin level ± sem, two-tailed Student's t test). (**d**) Cropped immunoblot and quantification of lamin A, progerin, and lamin C from $Lmna^{+/+}$ or $Lmna^{G609G/G609G}$ fibroblasts. Cells were incubated with vehicle or compound **21** at 2 μM for 14 days and then bafilomycin A (24 h at 25 nM) or MG-132 (5 h at 5 μM) was added when indicated ($n = 3$ independent experiments; plot shows mean ± sem, one-way ANOVA). (**e**) Cropped immunoblot and quantification of phosphorylated Akt (pAkt) and phosphorylated histone 2AX (pH2AX) from wild type (WT) or HGPS human fibroblasts incubated with vehicle or compound **21** at 2 μM for 10 days. Protein levels were normalized against total Akt or GAPDH ($n \geq 3$ independent experiments; plot shows mean ± sem, one-way ANOVA). (**f**) Human WT or HGPS fibroblasts were incubated with vehicle or compound **21** at 2 μM for 15 days. The activity of senescence-associated (SA) β-galactosidase was determined by incubating the cells with fluorescein di-β-D-galactopyranoside (FDG) for 24 h and measuring the resultant fluorescein production ($n \geq 3$ independent experiments in triplicates; plot shows mean ± sem, two-tailed Student's t test). (**g**) $Lmna^{+/+}$ C57BL/6 mice ($n = 2$ females; $n = 2$ males per time point) were treated with compound **21** (intraperitoneal injection, 40 mg/kg), blood was extracted at different time points, and the compound concentration in serum was determined by high-performance liquid chromatography coupled to mass spectrometry.

https://doi.org/10.1021/acscentsci.0c01698
ACS Cent. Sci. 2021, 7, 1300−1310

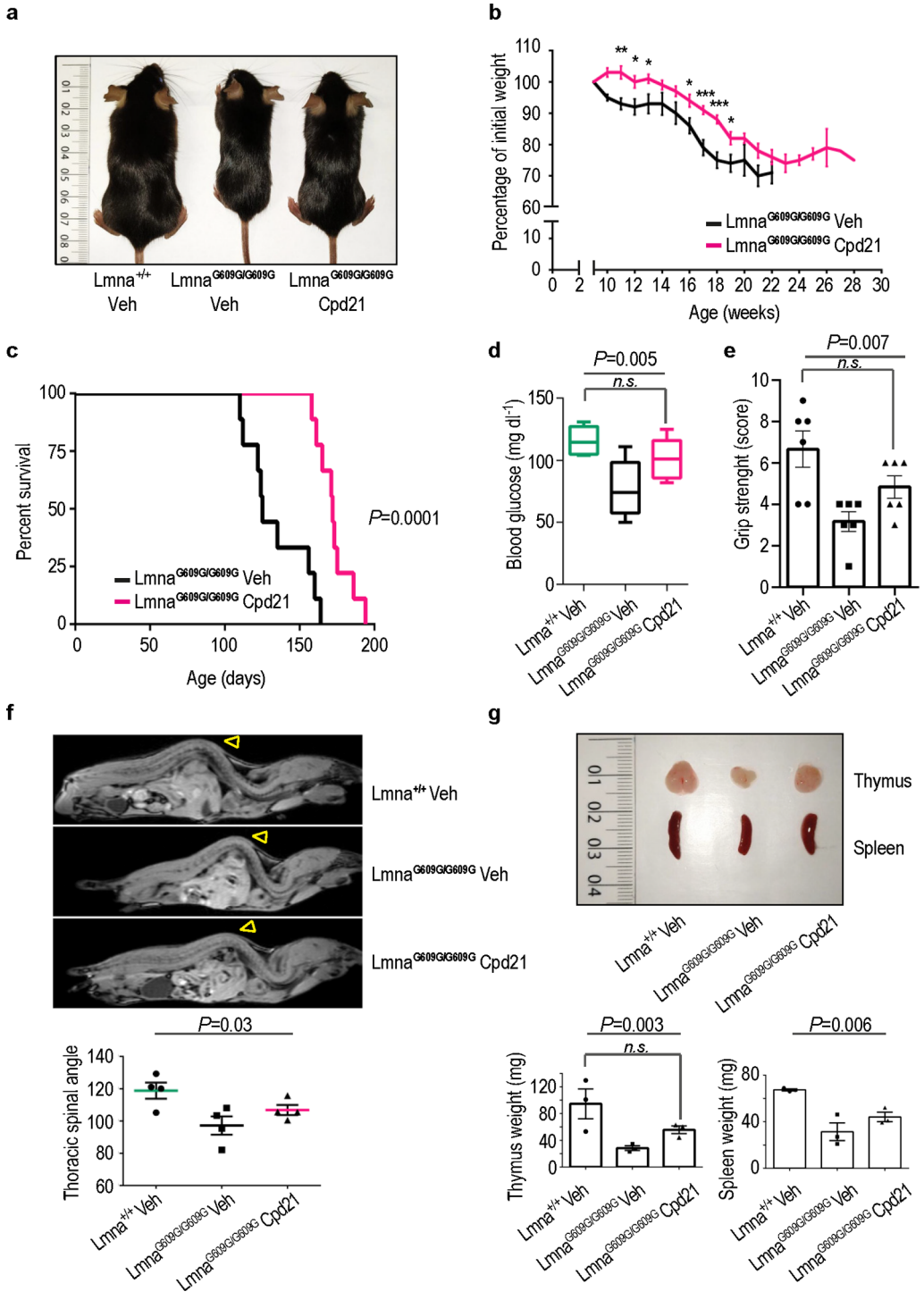

Figure 3. Improvement of the progeroid phenotype in vivo upon treatment with compound **21**. (**a**) Representative photograph of a 3-month-old *Lmna*$^{+/+}$ mouse, a *Lmna*$^{G609G/G609G}$ mouse, and a *Lmna*$^{G609G/G609G}$ mouse treated with compound **21** (40 mg/kg). (**b**) Body weight versus age plot of *Lmna*$^{G609G/G609G}$ mice treated with vehicle (n = 6) or with compound **21** (n = 9) (plot shows mean ± sem, two-tailed Student's t test, p-value * < 0.05, ** < 0.005, *** < 0.0005). (**c**) Kaplan–Meier survival plot showing a significant increase in life span in *Lmna*$^{G609G/G609G}$ mice treated with compound **21** (n = 9) compared with *Lmna*$^{G609G/G609G}$ mice treated with vehicle (n = 9) (P = 0.0001, log-rank/Mantel–Cox test). (**d**) Glycemia in *Lmna*$^{+/+}$ and *Lmna*$^{G609G/G609G}$ mice treated with compound **21** or vehicle (n = 6 per condition). Data are represented by box plots, and whiskers are minimum to maximum values (one-way ANOVA followed by Bonferroni–Holm post hoc test, n.s. non significant P = 0.11). (**e**) Grip strenght in *Lmna*$^{+/+}$ and *Lmna*$^{G609G/G609G}$ mice treated with compound **21** or vehicle (n = 5 per condition, one-way ANOVA followed by Bonferroni–Holm post hoc test, n.s. non significant P = 0.107). (**f**) Magnetic resonance imaging of a 3-month-old *Lmna*$^{+/+}$ mouse, a vehicle-treated *Lmna*$^{G609G/G609G}$ mouse, and a compound **21**-treated *Lmna*$^{G609G/G609G}$ mouse. Note that the marked curvature of the spine called lordokyphosis, a key feature of progeria, is reduced upon treatment with compound **21**. The plot represents the average of inner column angle (yellow arrowhead) of ≥4 mice per condition (one-way ANOVA). (**g**) Representative photographs of thymus and spleen from a 3-month-old *Lmna*$^{+/+}$ mouse, a vehicle-treated *Lmna*$^{G609G/G609G}$ mouse, and a compound **21**-treated *Lmna*$^{G609G/G609G}$ mouse. Plots represent average of thymus or spleen weight from ≥3 mice per condition (one-way ANOVA followed by Bonferroni–Holm post hoc test, n.s. non significant P = 0.17).

https://doi.org/10.1021/acscentsci.0c01698
ACS Cent. Sci. 2021, 7, 1300–1310

progeroid cells (Figure 1f). In addition, the phosphorylated levels of histone H2AX, a marker of nuclear damage associated with aging,[21] were also significantly reduced in the presence of compounds **14**, **17**, and **21**. Finally, no significant effect was observed in the number of misshapen nuclei in cells treated with these compounds (Supporting Figure S4). This is in agreement with the results reported in the ICMT genetically deficient mouse model.[16] Taken together, these results demonstrate that the new ICMT inhibitors described here significantly ameliorate the main cellular hallmarks of HGPS in progeroid fibroblasts from both $Lmna^{G609G/G609G}$ mice and HGPS patients, suggesting their potential for the treatment of the disease.

Selection of Compound 21 (UCM-13207) for In-Depth Studies. Among the three tested compounds, derivative **21** (UCM-13207) systematically induced the strongest effect in all the functional assays and showed a good IC_{50} value of 1.4 μM (Supporting Figure S5) in the ICMT in vitro assay. Compound **21** was also able to inhibit the ICMT activity in whole cells, as confirmed by prelamin accumulation in $Lmna^{+/+}$ cells (Supporting Figure S6), accumulation of carboxymethylated acetylfarnesylcysteine (the minimal substrate recognized by ICMT), and Ras mislocalization in $Lmna^{G609G/G609G}$ cells (Supporting Figure S7). Hence, it was selected for further exploration of its toxicity-efficacy window in vitro and key pharmacokinetic parameters before extending its evaluation to in vivo efficacy assessment using a mouse model of progeria. UCM-13207 did not cause appreciable cellular toxicity at least up to 10 μM (Figure 2a), whereas its efficacy to preserve the proliferation of progeroid cells was dose-dependent, with 2 μM showing the maximal effect (Figure 2b). Consistent with these results, compound **21** at 2 and 10 μM induced a decrease in progerin level (Figures 2c and 1d and e) without significantly affecting levels of wild-type lamin A and lamin C (Supporting Figure S8). The decrease in progerin levels seemed to be mediated by the proteasome pathway since blocking its activity with the specific inhibitor MG-132 reversed the effects of compound **21**, whereas treatment with the lysosome pathway inhibitor bafilomycin A did not significantly affect progerin down-regulation induced by compound **21** (Figure 2d). Cycloheximide turnover studies indicated the ability of the compound to exert a reduction in half-life of progerin (Supporting Figure S9). The decrease in total levels of progerin was not initially expected, since the effect of an ICMT inhibitor should be mainly the mislocalization of progerin from the nuclear rim and increased progerin levels have been reported in HGPS cells treated with C75, another ICMT inhibitor.[17] However, our results consistently showed decreased progerin levels both in human (Figure 1d) and mouse cells (Figures 1e, 2c, 2d, and Supporting Figure S3) treated with derivative **21**. We hypothesize that the extent of progerin mislocalization produced by the compound (around 36% for derivative **21** compared to vehicle as shown in Figure 1d) may be an important factor that contributes to decrease stability of progerin and to make it more prone to proteasome degradation. This effect has been observed for other inhibitors of the interaction between progerin and lamin A/C, such as compounds JH4 and SLC-DO11.[22,23] Both compounds induce a reduction in progerin levels that is reversed in the presence of a proteasome inhibitor, and a decrease in the half-life of progerin in experiments using cycloheximide. These results are in line with the findings reported here.

Moreover, human HGPS fibroblasts treated with compound **21** at 2 μM significantly increased phospho-Akt, reduced phospho-H2AX levels (Figure 2e) and diminished the levels of senescence-associated (SA) β-galactosidase activity (Figure 2f), a biomarker of senescent cells.[24]

With respect to the pharmacokinetic parameters, we first determined the cell culture and serum stability, the intrinsic clearance, and the serum free drug or fraction unbound (Fu) of the compound. Our in vitro stability results indicated excellent values for the half-life of compound **21** in both human and mouse cell culture media as well as in human serum ($t_{1/2}$ > 24 h), although a more moderate value was obtained in the case of mouse serum ($t_{1/2}$ = 29 ± 2 min). The in vitro microsomal intrinsic clearance was 40 ± 6 μL/min/mg protein in human samples and 144 ± 29 μL/min/mg protein in mouse samples. These values are predictive of a medium and high in vivo clearance, respectively, but since the Fu of compound **21** was 0.02 (with a K_D value for human serum albumin of 7.2 μM), this might reduce the metabolic clearance by the liver and, in turn, increase its half-life. Indeed, the in vivo half-life curve after intraperitoneal (ip) administration showed a significant and sustained concentration of the compound up to 6 h postadministration, reaching a maximum concentration close to 40 μM after 5 h (Figure 2g). In addition, signs of acute toxicity, tissue, or pathological damage were not detected at doses up to 80 mg/kg of compound **21**.

Compound 21 (UCM-13207) Improved the Overall Phenotype of Progeroid $Lmna^{G609G/G609G}$ Mice and Improved Cardiac Tissue Condition. Having demonstrated the in vitro efficacy of compound **21** in mouse and human progeroid cells, we evaluated its therapeutic potential in the progeroid $Lmna^{G609G/G609G}$ mice, a model that recapitulates the majority of the alterations observed in HGPS patients.[25−28]

Remarkably, progeroid mice treated with the ICMT inhibitor **21** showed significantly improved body weight at all ages tested (Figures 3a,b) and increased survival (Figure 3c). Thus, the mean survival of mice treated with the compound was extended to 173 days compared to 134 days of the vehicle treated mice (P = 0.0001, Figure 3c). Furthermore, the maximum survival increased from 164 to 194 days while the minimum survival from 110 to 158 days between untreated and treated animals, respectively. The beneficial effects of compound **21** were observed in both males and females (Supporting Figures S10−S12). Moreover, no signs of toxicity were observed in wild-type mice receiving the same dose of compound (Supporting Figure S13). Encouraged by these results, we explored other phenotypic features characteristic of the $Lmna^{G609G/G609G}$ progeria model such as reduced serum glucose levels, reduced grip strength, bone defects, and marked involutions of thymus and spleen.[25] Treatment of progeroid mice with compound **21** increased serum glucose levels and grip strength close to the values observed in wild-type controls (Figures 3d, e). Additionally, administration of the compound slightly improved lordokyphosis (abnormal convexity in the curvature of the spine when viewed from the side), increased spleen size (Figures 3f, g), and significantly increased the size of the thymus (Figure 3g).

Cardiovascular cells and tissues are major targets of progerin in animal models and in humans, being cardiovascular problems the main cause of death in progeria patients.[2,27,29−31] As such, specific decrease of progerin accumulation in cardiovascular tissues could be critical in maintaining the cardiovascular wellbeing. In line with this notion, treatment of

https://doi.org/10.1021/acscentsci.0c01698
ACS Cent. Sci. 2021, 7, 1300−1310

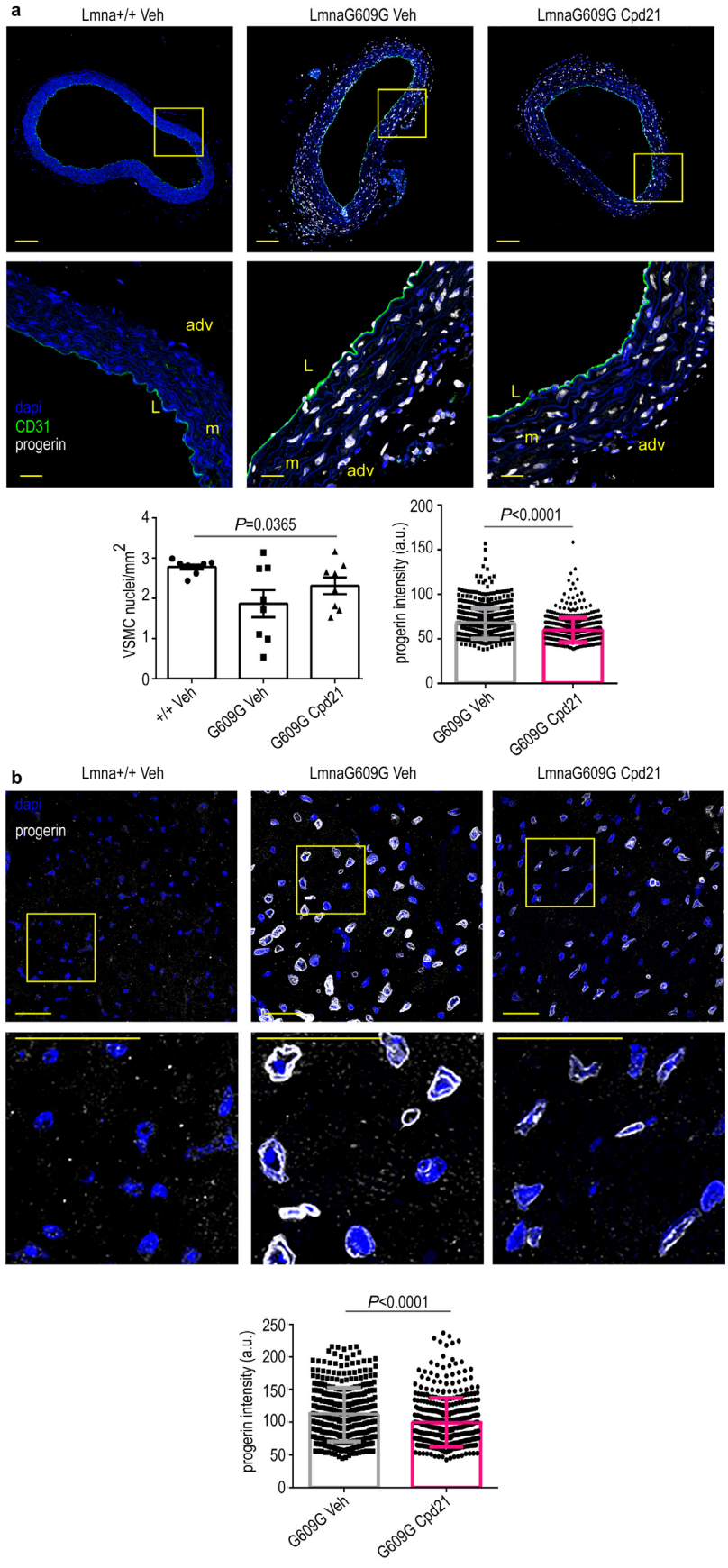

Figure 4. Reduced progerin expression in progeric *Lmna*$^{G609G/G609G}$ mice treated with compound **21**. Mice of the indicated genotypes were treated with compound **21** or vehicle, starting at 6 weeks of age, and were sacrificed at 12 weeks of age. Cross sections of aortic arch and heart were stained with antiprogerin antibody (white) and Hoechst 33342 to visualize nuclei (blue). Representative immunofluorescence images are shown. (**a**) Aortic

https://doi.org/10.1021/acscentsci.0c01698
ACS Cent. Sci. 2021, 7, 1300−1310

Figure 4. continued

arch. Scale bar: 100 μm (entire image) and 20 μm (magnified view). L, lumen; m, media; adv, adventitia. The left plot shows mean ± sem number of VSMCs in the medial layer of the aortic arch (n = 4 animal per condition, 2 sections per animal). The right plot shows mean ± desvest of progerin signal intensity in VSMC from the medial layer of the aortic arch (n = 646 nuclei for $Lmna^{G609G/G609G}$ treated with vehicle and 532 nuclei for $Lmna^{G609G/G609G}$ treated with compound **21**, from 4 animals per condition, two-tailed Student's t test). (**b**) Endocardial tissue. The bottom plot shows mean ± desvest of progerin signal intensity (n = 400 nuclei for $Lmna^{G609G/G609G}$ treated with vehicle and 412 nuclei for $Lmna^{G609G/G609G}$ treated with compound **21**, from 5 animals per condition, two-tailed Student's t test). Scale bar: 25 μm.

$Lmna^{G609G/G609G}$ mice with compound **21** substantially reduced progerin expression and increased the number of vascular smooth muscle cells (VSMCs) in the aortic arch (Figure 4a). Progerin levels were also decreased in endocardial tissue (Figure 4b), although the reduction was less evident in arterioles (Supporting Figure S15). Nonetheless, these results are relevant considering that progerin expression in VSMCs has been described as the main cause of vessel contraction impairment observed in HGPS[32] and that VSMCs loss is an important hallmark of vascular disease in HGPS.[27] Accordingly, specific decrease of progerin in aortic arch and endocardial tissue, together with an increase in the number of VSMCs, highlights that compound **21** is able to correct some of the critical primary causes of the cardiovascular complications that lead to the early death of HGPS patients. Importantly, compound **21** decreased fibrosis and microvascular cell loss in the heart of progeroid mice (Supporting Figures S14 and S15). In addition, treatment of mice with compound **21** led to an improvement in global tissue senescence in other organs such as liver and kidney (Supporting Figure S16) as assessed by quantification of the levels of SA β-galactosidase activity.

CONCLUSION

Here, we report a novel strategy to reduce the anomalous accumulation of progerin in the nuclear rim membrane, which is considered to be the main cause of the fatal phenotype developed by HGPS patients. Specifically, we show that compound **21** (UCM-13207), a new ICMT inhibitor, significantly induces the mislocalization of progerin and reduces its protein expression level, leading to a substantial overall amelioration of the cellular hallmarks of progeria in both mouse and human cells. Importantly, treatment with compound **21** significantly improved the phenotype of progeroid $Lmna^{G609G/G609G}$ mice, including lifespan extension in both males and females. Collectively, these findings have important clinical implications regarding the validation of the clinical relevance of ICMT as a promising therapeutic target for progeria treatment, providing a new pharmacological strategy in a field dramatically devoid of validated therapeutic targets beyond farnesyltransferase. Furthermore, our results pave the way for targeting ICMT as a new pharmacological strategy for succeeding in the long sought objective of making a meaningful difference to the lives of HGPS patients.

MATERIALS AND METHODS

Safety statement. No unexpected or unusually high safety hazards were encountered.

Compound Syntheses. The synthesis and structural characterization of compound **21** (UCM-13207) is detailed below. Full details regarding the synthetic procedures and characterization data of all compounds are given in the Supporting Information.

Synthesis of N^2-Octyl-N^1-phenyl-N^2-(pyridin-2-ylcarbonyl)-β-alaninamide (21, UCM-13207). To a solution of picolinic acid (133 mg, 1.1 mmol) in anhydrous DCM (4 mL/mmol), EDC (207 mg, 1.1 mmol) and HOBt (146 mg, 1.1 mmol) were added. The reaction mixture was stirred at rt for 1 h. Then, a solution of N^2-octyl-N^1-phenyl-β-alaninamide (150 mg, 0.54 mmol) in anhydrous DCM (2.0 mL/mmol) was added and the reaction mixture was stirred at rt for 16 h. The reaction crude was washed with saturated aqueous solutions of $NaHCO_3$ and NaCl, consecutively. The organic extracts were dried over Na_2SO_4, filtered, and the solvent was removed under reduced pressure. The residue was purified by column chromatography (hexane/EtOAc, 2:8) to yield compound **21** in 92% yield (189 mg).

R_f (hexane/EtOAc, 3:7): 0.30. IR (ATR, cm^{-1}): 3309 (NH), 1685 (CON), 1615, 1547, 1495, 1443 (Ar). ^{1}H NMR ($CDCl_3$, δ): Amide rotamers A:B, 2:1; 0.85 (t, J = 6.7 Hz, 3H, CH_3), 1.11−1.25 (m, 10H, $(CH_2)_5CH_3$), 1.57 (m, 2H, $CH_2(CH_2)_5CH_3$), 2.81 (t, J = 6.4 Hz, 2H, CH_2CO), 3.37 (t, J = 7.4 Hz, 2H, $(CH_2)_6CH_2N$, rotamer A), 3.46−3.47 (m, 2H, $(CH_2)_6CH_2N$, rotamer B), 3.69−3.75 (m, 2H, $COCH_2CH_2N$, rotamer B), 3.87 (t, J = 6.3 Hz, 2H, $COCH_2CH_2N$, rotamer A), 7.05 (t, J = 7.1 Hz, 1H, H_4), 7.24−7.32 (m, 3H, H_3, H_5, $H_{5'}$), 7.54−7.56 (m, 3H, H_2, H_6, $H_{4'}$), 7.71−7.76 (m, 1H, $H_{3'}$), 8.55 (d, J = 4.4 Hz, 1H, $H_{6'}$), 8.64 (br s, 1H, NH, rotamer B), 8.92 (br s, 1H, NH, rotamer A). ^{13}C NMR ($CDCl_3$, δ): 14.0 (CH_3), 22.6, 26.5, 28.8, 29.0 (2C), 31.7 ($(CH_2)_6CH_3$), 36.5 (CH_2CO), 43.2 (CH_2N), 50.0 ($(CH_2)_6CH_2N$), 119.9 (C_2, C_6), 123.1, 123.9, 124.4 (C_4, $C_{3'}$, $C_{5'}$), 128.8 (C_3, C_5), 137.0 ($C_{4'}$), 138.4 (C_1), 148.5 ($C_{6'}$), 154.5 ($C_{2'}$), 169.5, 169.7 (CONH, CON). HRMS (ESI, m/z): Calculated for $C_{23}H_{31}N_3O_2Na$ $[M + Na]^+$: 404.2308. Found: 404.2276.

Determination of ICMT Activity. Synthesized compounds were tested for their ability to inhibit human ICMT activity using Sf9 membranes containing the recombinantly expressed enzyme. In this assay, a mixture of biotin-farnesyl-L-cysteine and tritiated S-adenosylmethionine in the presence or absence of the compound under study was prepared, and the reaction was initiated by the addition of the Sf9 membrane homogenates. The inhibitory capacity of the compounds was expressed as percentage of inhibition of the methyl esterification step, in which the tritiated methyl group of the methyl donor S-adenosylmethionine was transferred to the substrate biotin-farnesyl-L-cysteine as described previously,[33] and the radioactivity incorporated was quantified.

Cell Lines and Culture. Progeroid mouse fibroblasts ($Lmna^{G609/G609}$) and their wild-type counterparts were kindly donated by Prof. Carlos López Otín (Oviedo University, Spain). Cells were grown in Dulbecco's modified eagle medium (DMEM, Invitrogen) supplemented with 10% heat-inactivated fetal bovine serum (FBS, HyClone), 1% L-glutamine (Invitrogen), 1% sodium pyruvate (Invitrogen), 50 U/mL penicillin, and 50 μg/mL streptomycin (Invitrogen). Human progeroid or healthy fibroblasts (HGADFN167,

https://doi.org/10.1021/acscentsci.0c01698
ACS Cent. Sci. 2021, 7, 1300−1310

HGADFN003, HGADFN143, and HGFDFN168) were obtained from The Progeria Research Foundation and cultured in 15% DMEM, 50 U/mL penicillin and 50 μg/mL streptomycin. All cells were incubated in a humidified atmosphere at 37 °C in the presence of 5% CO_2.

Cell Viability and Proliferation Assays. The effect of the different compounds on the cellular viability was determined through standard MTT assays.[34−36] Full details are given in the Supporting Information.

RNA Interference-Mediated Silencing of the ICMT Gene. Progeroid mouse fibroblasts ($Lmna^{G609/G609}$) were transfected with an ICMT siRNA (m) or with a control siRNA commercially available from Santa Cruz Biotechnology (sc-146137 and sc-37007, respectively), using lipofectamine and following the manufacturer's instructions. To determine cell viability, the MTT protocol indicated above was followed.

Immunoblot and Immunocytofluorescence Analysis. Western blot analysis was carried out as described previously.[37−39] Full details are given in the Supporting Information.

Senescence-Associated (SA) β-Galactosidase Activity. SA β-galactosidase activity was determined by the FDG method.[40] Full details are provided in the Supporting Information.

Stability Assays. Stability in cell culture medium, in mouse and human serum, and in mouse and human liver microsomes was assayed as detailed in the Supporting Information.

Human Serum Albumin (HSA) Binding Assay. Determination of the binding of the compound to HSA was performed by incubating a fixed concentration of the compound with different concentrations of immobilized HSA, using the TRANSILXL HSA Binding Kit (TMP-0210-2096, Sovicell) as described in the Supporting Information.

Animal Experiments. All scientific procedures with animals were conformed to EU Directive 2010/63 EU and Recommendation 2007/526/EC, enforced in Spanish law under Real Decreto 53/2013. Animal protocols were approved by the Committee of Animal Experimentation of Universidad Complutense de Madrid and the Animal Protection Area of the Comunidad Autónoma de Madrid (PROEX 159/18). Animal studies were carried out in $Lmna^{G609G/G609G}$ knock-in mice ubiquitously expressing progerin[25] and control $Lmna^{+/+}$ littermates. Mice were maintained in the animal facility of the Universidad Complutense de Madrid under specific pathogen free conditions. Full details about the in vivo characterization and the pathological and immunohistofluorescence analysis are provided in the Supporting Information.

Statistics. All data were analyzed using GraphPad Prism 6 software. Data were presented as mean ± standard error of the media (SEM) with at least three biologically independent experiments. Representative morphological images were taken from at least three biologically independent experiments with similar results. The Student t test or one-way ANOVA were used for comparison between groups. Survival analysis was performed using the Kaplan−Meier method. Differences between survival distributions were analyzed using the log rank test. Hazard ratio and confidence interval were obtained by Mantel−Haenszel analysis. Differences with $P < 0.05$ were considered significant.

■ ASSOCIATED CONTENT

Supporting Information

The Supporting Information is available free of charge at https://pubs.acs.org/doi/10.1021/acscentsci.0c01698.

Supporting Table S1, Supporting Figures showing the effect of compounds in the viability of $Lmna^{+/+}$ or $Lmna^{G609G/G609G}$ mouse fibroblasts; lack of effect of compound **21** in the viability of siRNA-induced silencing of ICMT $Lmna^{G609G/G609G}$ mouse fibroblasts, on misshapen nuclei, and in lamin A or lamin C levels; concentration−response curve for ICMT inhibition of compound **21**; effect of compound **21** in the total levels of progerin, in prelamin accumulation in $Lmna^{+/+}$ cells, in Ras mislocalization, and in methylated acetyl-farnesylcysteine accumulation in $Lmna^{G609G/G609G}$ cells; half-life of progerin in the presence of cycloheximide; size, body weight, and survival improvement in male and female progeroid mice after administration of compound **21**; lack of in vivo toxicity of compound **21** in male and female mice; reduction of heart fibrosis and microvascular cell loss in progeroid mice treated with compound **21**; SA β-galactosidase activity in kidney and liver of progeroid treated mice; detailed synthetic methods; full details for cell viability and proliferation assays, for immunoblot and immunocytofluorescence analysis, for SA β-galactosidase activity determination, for stability, and human serum albumin binding assay, for the in vivo studies, for the pathological and immunofluorescence analysis, and for the determination of the levels of methylated AFC in cells (PDF)

■ AUTHOR INFORMATION

Corresponding Author

Silvia Ortega-Gutiérrez − *Departamento de Química Orgánica, Facultad de Ciencias Químicas, Universidad Complutense de Madrid, E-28040 Madrid, Spain;* orcid.org/0000-0002-0257-6754; Email: siortega@ucm.es

Authors

Beatriz Marcos-Ramiro − *Departamento de Química Orgánica, Facultad de Ciencias Químicas, Universidad Complutense de Madrid, E-28040 Madrid, Spain*

Ana Gil-Ordóñez − *Departamento de Química Orgánica, Facultad de Ciencias Químicas, Universidad Complutense de Madrid, E-28040 Madrid, Spain*

Nagore I. Marín-Ramos − *Departamento de Química Orgánica, Facultad de Ciencias Químicas, Universidad Complutense de Madrid, E-28040 Madrid, Spain; CEI Campus Moncloa, UCM-UPM and CSIC, E-28040 Madrid, Spain*

Francisco J. Ortega-Nogales − *Departamento de Química Orgánica, Facultad de Ciencias Químicas, Universidad Complutense de Madrid, E-28040 Madrid, Spain*

Moisés Balabasquer − *Departamento de Química Orgánica, Facultad de Ciencias Químicas, Universidad Complutense de Madrid, E-28040 Madrid, Spain*

Pilar Gonzalo − *Vascular Pathophysiology Area, Centro Nacional de Investigaciones Cardiovasculares (CNIC), E-28029 Madrid, Spain; Centro de Investigación Biomédica en Red de Enfermedades Cardiovasculares (CIBERCV), 28029 Madrid, Spain*

Nora Khiar-Fernández − *Departamento de Química Orgánica, Facultad de Ciencias Químicas, Universidad Complutense de Madrid, E-28040 Madrid, Spain*
Loïc Rolas − *Centre for Microvascular Research, William Harvey Research Institute, Barts and The London School of Medicine and Dentistry, Queen Mary University of London, London EC1M 6BQ, United Kingdom*
Anna Barkaway − *Centre for Microvascular Research, William Harvey Research Institute, Barts and The London School of Medicine and Dentistry, Queen Mary University of London, London EC1M 6BQ, United Kingdom*
Sussan Nourshargh − *Centre for Microvascular Research, William Harvey Research Institute, Barts and The London School of Medicine and Dentistry, Queen Mary University of London, London EC1M 6BQ, United Kingdom*
Vicente Andrés − *Vascular Pathophysiology Area, Centro Nacional de Investigaciones Cardiovasculares (CNIC), E-28029 Madrid, Spain; Centro de Investigación Biomédica en Red de Enfermedades Cardiovasculares (CIBERCV), 28029 Madrid, Spain*
Mar Martín-Fontecha − *Departamento de Química Orgánica, Facultad de Ciencias Químicas, Universidad Complutense de Madrid, E-28040 Madrid, Spain*
María L. López-Rodríguez − *Departamento de Química Orgánica, Facultad de Ciencias Químicas, Universidad Complutense de Madrid, E-28040 Madrid, Spain;* orcid.org/0000-0001-8607-1085

Complete contact information is available at: https://pubs.acs.org/10.1021/acscentsci.0c01698

Notes

The authors declare no competing financial interest.

■ ACKNOWLEDGMENTS

This work was supported by grants from The Progeria Research Foundation (PRF 2016-65) and the Spanish MINECO (PID2019-106279RB-I00, PID2019-108489RB-I00). The authors thank Fundación La Caixa (A.G.), CEI Moncloa (N.I.M.-R.), MINECO (F.J.O.-N. and M.B.) and Ministerio de Ciencia, Innovación y Universidades (N.K.-F.) for predoctoral fellowships. The authors thank C. López-Otín for kindly donating $Lmna^{G609G/G609G}$ progeroid and their corresponding wild-type fibroblasts and UCM's CAIs Cytometry and Fluorescence Microscopy, Genomics, NMR, and Mass Spectrometry, for their assistance. The CNIC is supported by the Ministerio de Ciencia e Innovación, the Instituto de Salud Carlos III, and the pro-CNIC Foundation, and is a Severo Ochoa Center of Excellence (grant SEV-2015-0505). The generation of the antiprogerin antibody was funded by the Wellcome Trust (098291/Z/12/Z to S.N.).

■ REFERENCES

(1) Gordon, L. B.; Rothman, F. G.; Lopez-Otin, C.; Misteli, T. Progeria: a paradigm for translational medicine. *Cell* **2014**, *156*, 400−407.
(2) Dorado, B.; Andres, V. A-type lamins and cardiovascular disease in premature aging syndromes. *Curr. Opin. Cell Biol.* **2017**, *46*, 17−25.
(3) Merideth, M. A.; Gordon, L. B.; Clauss, S.; Sachdev, V.; Smith, A. C.; Perry, M. B.; Brewer, C. C.; Zalewski, C.; Kim, H. J.; Solomon, B.; Brooks, B. P.; Gerber, L. H.; Turner, M. L.; Domingo, D. L.; Hart, T. C.; Graf, J.; Reynolds, J. C.; Gropman, A.; Yanovski, J. A.; Gerhard-Herman, M.; Collins, F. S.; Nabel, E. G.; Cannon, R. O., 3rd; Gahl, W. A.; Introne, W. J. Phenotype and course of Hutchinson-Gilford progeria syndrome. *N. Engl. J. Med.* **2008**, *358*, 592−604.
(4) Eriksson, M.; Brown, W. T.; Gordon, L. B.; Glynn, M. W.; Singer, J.; Scott, L.; Erdos, M. R.; Robbins, C. M.; Moses, T. Y.; Berglund, P.; Dutra, A.; Pak, E.; Durkin, S.; Csoka, A. B.; Boehnke, M.; Glover, T. W.; Collins, F. S. Recurrent de novo point mutations in lamin A cause Hutchinson-Gilford progeria syndrome. *Nature* **2003**, *423*, 293−298.
(5) De Sandre-Giovannoli, A.; Bernard, R.; Cau, P.; Navarro, C.; Amiel, J.; Boccaccio, I.; Lyonnet, S.; Stewart, C. L.; Munnich, A.; Le Merrer, M.; Levy, N. Lamin A truncation in Hutchinson-Gilford progeria. *Science* **2003**, *300*, 2055.
(6) Davies, B. S.; Fong, L. G.; Yang, S. H.; Coffinier, C.; Young, S. G. The posttranslational processing of prelamin A and disease. *Annu. Rev. Genomics Hum. Genet.* **2009**, *10*, 153−174.
(7) Gordon, L. B.; Shappell, H.; Massaro, J.; D'Agostino, R. B., Sr.; Brazier, J.; Campbell, S. E.; Kleinman, M. E.; Kieran, M. W. Association of lonafarnib treatment vs no treatment with mortality rate in patients with Hutchinson-Gilford progeria syndrome. *Jama* **2018**, *319*, 1687−1695.
(8) Varela, I.; Pereira, S.; Ugalde, A. P.; Navarro, C. L.; Suarez, M. F.; Cau, P.; Cadinanos, J.; Osorio, F. G.; Foray, N.; Cobo, J.; de Carlos, F.; Levy, N.; Freije, J. M.; Lopez-Otin, C. Combined treatment with statins and aminobisphosphonates extends longevity in a mouse model of human premature aging. *Nat. Med.* **2008**, *14*, 767−772.
(9) Gordon, L. B.; Kleinman, M. E.; Massaro, J.; D'Agostino, R. B., Sr.; Shappell, H.; Gerhard-Herman, M.; Smoot, L. B.; Gordon, C. M.; Cleveland, R. H.; Nazarian, A.; Snyder, B. D.; Ullrich, N. J.; Silvera, V. M.; Liang, M. G.; Quinn, N.; Miller, D. T.; Huh, S. Y.; Dowton, A. A.; Littlefield, K.; Greer, M. M.; Kieran, M. W. Clinical trial of the protein farnesylation inhibitors lonafarnib, pravastatin, and zoledronic acid in children with Hutchinson-Gilford progeria syndrome. *Circulation* **2016**, *134*, 114−125.
(10) Marin-Ramos, N. I.; Ortega-Gutierrez, S.; Lopez-Rodriguez, M. L. Blocking Ras inhibition as an antitumor strategy. *Semin. Cancer Biol.* **2019**, *54*, 91−100.
(11) Balmus, G.; Larrieu, D.; Barros, A. C.; Collins, C.; Abrudan, M.; Demir, M.; Geisler, N. J.; Lelliott, C. J.; White, J. K.; Karp, N. A.; Atkinson, J.; Kirton, A.; Jacobsen, M.; Clift, D.; Rodriguez, R.; Adams, D. J.; Jackson, S. P. Targeting of NAT10 enhances healthspan in a mouse model of human accelerated aging syndrome. *Nat. Commun.* **2018**, *9*, 1700.
(12) Santiago-Fernandez, O.; Osorio, F. G.; Quesada, V.; Rodriguez, F.; Basso, S.; Maeso, D.; Rolas, L.; Barkaway, A.; Nourshargh, S.; Folgueras, A. R.; Freije, J. M. P.; Lopez-Otin, C. Development of a CRISPR/Cas9-based therapy for Hutchinson-Gilford progeria syndrome. *Nat. Med.* **2019**, *25*, 423−426.
(13) Beyret, E.; Liao, H. K.; Yamamoto, M.; Hernandez-Benitez, R.; Fu, Y.; Erikson, G.; Reddy, P.; Izpisua-Belmonte, J. C. Single-dose CRISPR-Cas9 therapy extends lifespan of mice with Hutchinson-Gilford progeria syndrome. *Nat. Med.* **2019**, *25*, 419−422.
(14) Barcena, C.; Valdes-Mas, R.; Mayoral, P.; Garabaya, C.; Durand, S.; Rodriguez, F.; Fernandez-Garcia, M. T.; Salazar, N.; Nogacka, A. M.; Garatachea, N.; Bossut, N.; Aprahamian, F.; Lucia, A.; Kroemer, G.; Freije, J. M. P.; Quiros, P. M.; Lopez-Otin, C. Healthspan and lifespan extension by fecal microbiota transplantation into progeroid mice. *Nat. Med.* **2019**, *25*, 1234−1242.
(15) Villa-Bellosta, R. ATP-based therapy prevents vascular calcification and extends longevity in a mouse model of Hutchinson-Gilford progeria syndrome. *Proc. Natl. Acad. Sci. U. S. A.* **2019**, *116*, 23698−23704.
(16) Ibrahim, M. X.; Sayin, V. I.; Akula, M. K.; Liu, M.; Fong, L. G.; Young, S. G.; Bergo, M. O. Targeting isoprenylcysteine methylation ameliorates disease in a mouse model of progeria. *Science* **2013**, *340*, 1330−1333.
(17) Chen, X.; Yao, H.; Kashif, M.; Revêchon, G.; Eriksson, M.; Hu, J.; Wang, T.; Liu, Y.; Tüksammel, E.; Strömblad, S.; Ahearn, I. M.; Philips, M. R.; Wiel, C.; Ibrahim, M. X.; Bergo, M. O. A small-

molecule ICMT inhibitor delays senescence of Hutchinson-Gilford progeria syndrome cells. *eLife* **2021**, DOI: 10.7554/eLife.63284.
(18) Bertozzi, C. R.; Chang, C. J.; Davis, B. G.; Olvera de la Cruz, M.; Tirrell, D. A.; Zhao, D. Grand challenges in chemistry for 2016 and beyond. *ACS Cent. Sci.* **2016**, *2*, 1−3.
(19) López-Rodríguez, M. L.; Ortega-Gutiérrez, S.; Martín-Fontecha, M.; Balabasquer, M.; Ortega-Nogales, F. J.; Marín-Ramos, N. I. Novel Inhibitors of the Enzyme Isoprenylcysteine Carboxyl Methyltransferase (ICMT). WO2014118418A1, 2014.
(20) Marin-Ramos, N. I.; Balabasquer, M.; Ortega-Nogales, F. J.; Torrecillas, I. R.; Gil-Ordonez, A.; Marcos-Ramiro, B.; Aguilar-Garrido, P.; Cushman, I.; Romero, A.; Medrano, F. J.; Gajate, C.; Mollinedo, F.; Philips, M. R.; Campillo, M.; Gallardo, M.; Martin-Fontecha, M.; Lopez-Rodriguez, M. L.; Ortega-Gutierrez, S. A potent isoprenylcysteine carboxylmethyltransferase (ICMT) inhibitor improves survival in Ras-driven acute myeloid leukemia. *J. Med. Chem.* **2019**, *62*, 6035−6046.
(21) Ocampo, A.; Reddy, P.; Martinez-Redondo, P.; Platero-Luengo, A.; Hatanaka, F.; Hishida, T.; Li, M.; Lam, D.; Kurita, M.; Beyret, E.; Araoka, T.; Vazquez-Ferrer, E.; Donoso, D.; Roman, J. L.; Xu, J.; Rodriguez Esteban, C.; Nunez, G.; Nunez Delicado, E.; Campistol, J. M.; Guillen, I.; Guillen, P.; Izpisua Belmonte, J. C. In vivo amelioration of age-associated hallmarks by partial reprogramming. *Cell* **2016**, *167*, 1719−1733.
(22) Lee, S. J.; Jung, Y. S.; Yoon, M. H.; Kang, S. M.; Oh, A. Y.; Lee, J. H.; Jun, S. Y.; Woo, T. G.; Chun, H. Y.; Kim, S. K.; Chung, K. J.; Lee, H. Y.; Lee, K.; Jin, G.; Na, M. K.; Ha, N. C.; Barcena, C.; Freije, J. M.; Lopez-Otin, C.; Song, G. Y.; Park, B. J. Interruption of progerin-lamin A/C binding ameliorates Hutchinson-Gilford progeria syndrome phenotype. *J. Clin. Invest.* **2016**, *126*, 3879−3893.
(23) Kang, S. M.; Yoon, M. H.; Ahn, J.; Kim, J. E.; Kim, S. Y.; Kang, S. Y.; Joo, J.; Park, S.; Cho, J. H.; Woo, T. G.; Oh, A. Y.; Chung, K. J.; An, S. Y.; Hwang, T. S.; Lee, S. Y.; Kim, J. S.; Ha, N. C.; Song, G. Y.; Park, B. J. Progerinin, an optimized progerin-lamin A binding inhibitor, ameliorates premature senescence phenotypes of Hutchinson-Gilford progeria syndrome. *Commun. Biol.* **2021**, *4*, 1.
(24) Debacq-Chainiaux, F.; Erusalimsky, J. D.; Campisi, J.; Toussaint, O. Protocols to detect senescence-associated beta-galactosidase (SA-betagal) activity, a biomarker of senescent cells in culture and in vivo. *Nat. Protoc.* **2009**, *4*, 1798−1806.
(25) Osorio, F. G.; Navarro, C. L.; Cadinanos, J.; Lopez-Mejia, I. C.; Quiros, P. M.; Bartoli, C.; Rivera, J.; Tazi, J.; Guzman, G.; Varela, I.; Depetris, D.; de Carlos, F.; Cobo, J.; Andres, V.; De Sandre-Giovannoli, A.; Freije, J. M.; Levy, N.; Lopez-Otin, C. Splicing-directed therapy in a new mouse model of human accelerated aging. *Sci. Transl. Med.* **2011**, *3*, 106ra107.
(26) Villa-Bellosta, R.; Rivera-Torres, J.; Osorio, F. G.; Acín-Pérez, R.; Enriquez, J. A.; López-Otín, C.; Andrés, V. Defective extracellular pyrophosphate metabolism promotes vascular calcification in a mouse model of Hutchinson-Gilford progeria syndrome that is ameliorated on pyrophosphate treatment. *Circulation* **2013**, *127*, 2442−2451.
(27) Hamczyk, M. R.; Villa-Bellosta, R.; Gonzalo, P.; Andres-Manzano, M. J.; Nogales, P.; Bentzon, J. F.; Lopez-Otin, C.; Andres, V. Vascular smooth muscle-specific progerin expression accelerates atherosclerosis and death in a mouse model of Hutchinson-Gilford progeria syndrome. *Circulation* **2018**, *138*, 266−282.
(28) Del Campo, L.; Sanchez-Lopez, A.; Salaices, M.; von Kleeck, R. A.; Exposito, E.; Gonzalez-Gomez, C.; Cusso, L.; Guzman-Martinez, G.; Ruiz-Cabello, J.; Desco, M.; Assoian, R. K.; Briones, A. M.; Andres, V. Vascular smooth muscle cell-specific progerin expression in a mouse model of Hutchinson-Gilford progeria syndrome promotes arterial stiffness: Therapeutic effect of dietary nitrite. *Aging Cell* **2019**, *18*, e12936.
(29) Hamczyk, M. R.; Villa-Bellosta, R.; Quesada, V.; Gonzalo, P.; Vidak, S.; Nevado, R. M.; Andrés-Manzano, M. J.; Misteli, T.; López-Otín, C.; Andrés, V. Progerin accelerates atherosclerosis by inducing endoplasmic reticulum stress in vascular smooth muscle cells. *EMBO Mol. Med.* **2019**, *11*, e9736.
(30) Osmanagic-Myers, S.; Kiss, A.; Manakanatas, C.; Hamza, O.; Sedlmayer, F.; Szabo, P. L.; Fischer, I.; Fichtinger, P.; Podesser, B. K.; Eriksson, M.; Foisner, R. Endothelial progerin expression causes cardiovascular pathology through an impaired mechanoresponse. *J. Clin. Invest.* **2019**, *129*, 531−545.
(31) Dorado, B.; Pløen, G. G.; Barettino, A.; Macías, A.; Gonzalo, P.; Andrés-Manzano, M. J.; González-Gómez, C.; Galán-Arriola, C.; Alfonso, J. M.; Lobo, M.; López-Martín, G. J.; Molina, A.; Sánchez-Sánchez, R.; Gadea, J.; Sánchez-González, J.; Liu, Y.; Callesen, H.; Filgueiras-Rama, D.; Ibáñez, B.; Sørensen, C. B.; Andrés, V. Generation and characterization of a novel knockin minipig model of Hutchinson-Gilford progeria syndrome. *Cell Discovery* **2019**, *5*, 16.
(32) Del Campo, L.; Sánchez-López, A.; González-Gómez, C.; Andrés-Manzano, M. J.; Dorado, B.; Andrés, V. Vascular smooth muscle cell-specific progerin expression provokes contractile impairment in a mouse model of Hutchinson-Gilford progeria syndrome that is ameliorated by nitrite treatment. *Cells* **2020**, *9*, 656.
(33) Winter-Vann, A. M.; Baron, R. A.; Wong, W.; dela Cruz, J.; York, J. D.; Gooden, D. M.; Bergo, M. O.; Young, S. G.; Toone, E. J.; Casey, P. J. A small-molecule inhibitor of isoprenylcysteine carboxyl methyltransferase with antitumor activity in cancer cells. *Proc. Natl. Acad. Sci. U. S. A.* **2005**, *102*, 4336−4341.
(34) Gamo, A. M.; Gonzalez-Vera, J. A.; Rueda-Zubiaurre, A.; Alonso, D.; Vazquez-Villa, H.; Martin-Couce, L.; Palomares, O.; Lopez, J. A.; Martin-Fontecha, M.; Benhamu, B.; Lopez-Rodriguez, M. L.; Ortega-Gutierrez, S. Chemoproteomic approach to explore the target profile of GPCR ligands: Application to 5-HT_{1A} and 5-HT_6 receptors. *Chem. - Eur. J.* **2016**, *22*, 1313−1321.
(35) Marin-Ramos, N. I.; Alonso, D.; Ortega-Gutierrez, S.; Ortega-Nogales, F. J.; Balabasquer, M.; Vazquez-Villa, H.; Andradas, C.; Blasco-Benito, S.; Perez-Gomez, E.; Canales, A.; Jimenez-Barbero, J.; Marquina, A.; Del Prado, J. M.; Sanchez, C.; Martin-Fontecha, M.; Lopez-Rodriguez, M. L. New inhibitors of angiogenesis with antitumor activity in vivo. *J. Med. Chem.* **2015**, *58*, 3757−3766.
(36) Marín-Ramos, N. I.; Piñar, C.; Vázquez-Villa, H.; Martín-Fontecha, M.; González, Á.; Canales, Á.; Algar, S.; Mayo, P. P.; Jiménez-Barbero, J.; Gajate, C.; Mollinedo, F.; Pardo, L.; Ortega-Gutiérrez, S.; Viso, A.; López-Rodríguez, M. L. Development of a nucleotide exchange inhibitor that impairs Ras oncogenic signaling. *Chem. - Eur. J.* **2017**, *23*, 1676−1685.
(37) Hernandez-Torres, G.; Cipriano, M.; Heden, E.; Bjorklund, E.; Canales, A.; Zian, D.; Feliu, A.; Mecha, M.; Guaza, C.; Fowler, C. J.; Ortega-Gutierrez, S.; Lopez-Rodriguez, M. L. A reversible and selective inhibitor of monoacylglycerol lipase ameliorates multiple sclerosis. *Angew. Chem., Int. Ed.* **2014**, *53*, 13765−13770.
(38) Hernandez-Torres, G.; Enriquez-Palacios, E.; Mecha, M.; Feliu, A.; Rueda-Zubiaurre, A.; Angelina, A.; Martin-Cruz, L.; Martin-Fontecha, M.; Palomares, O.; Guaza, C.; Pena-Cabrera, E.; Lopez-Rodriguez, M. L.; Ortega-Gutierrez, S. Development of a fluorescent bodipy probe for visualization of the serotonin 5-HT1A receptor in native cells of the immune system. *Bioconjugate Chem.* **2018**, *29*, 2021−2027.
(39) Turrado, C.; Puig, T.; García-Cárceles, J.; Artola, M.; Benhamú, B.; Ortega-Gutiérrez, S.; Relat, J.; Oliveras, G.; Blancafort, A.; Haro, D.; Marrero, P. F.; Colomer, R.; López-Rodríguez, M. L. New synthetic inhibitors of fatty acid synthase with anticancer activity. *J. Med. Chem.* **2012**, *55*, 5013−5023.
(40) Yang, N. C.; Hu, M. L. A fluorimetric method using fluorescein di-beta-D-galactopyranoside for quantifying the senescence-associated beta-galactosidase activity in human foreskin fibroblast Hs68 cells. *Anal. Biochem.* **2004**, *325*, 337−343.

https://doi.org/10.1021/acscentsci.0c01698
ACS Cent. Sci. 2021, 7, 1300−1310